



HAL
open science

From Behavior of Water on Hydrophobic Graphene Surfaces to Ultra-Confinement of Water in Carbon Nanotubes

Alia Mejri, Guillaume Herlem, Fabien Picaud

► **To cite this version:**

Alia Mejri, Guillaume Herlem, Fabien Picaud. From Behavior of Water on Hydrophobic Graphene Surfaces to Ultra-Confinement of Water in Carbon Nanotubes. *Nanomaterials*, 2021, 11 (2), pp.306. 10.3390/nano11020306 . hal-04189066

HAL Id: hal-04189066

<https://hal.science/hal-04189066>

Submitted on 28 Aug 2023

HAL is a multi-disciplinary open access archive for the deposit and dissemination of scientific research documents, whether they are published or not. The documents may come from teaching and research institutions in France or abroad, or from public or private research centers.

L'archive ouverte pluridisciplinaire **HAL**, est destinée au dépôt et à la diffusion de documents scientifiques de niveau recherche, publiés ou non, émanant des établissements d'enseignement et de recherche français ou étrangers, des laboratoires publics ou privés.

1 Article

2 **From behavior of water on hydrophobic graphene surface to ul-**
3 **tra-confinement of water in carbon nanotube**4 **Alia MEJRI¹, Guillaume HERLEM¹ and Fabien PICAUD ^{1,*}**5 ¹ Laboratoire de Nanomédecine, Imagerie et Thérapeutiques, EA4662, UFR Sciences et Techniques, Centre
6 Hospitalier Universitaire et Université de Bourgogne Franche Comté, 16 route de Gray, 25030 Besançon

7 * Correspondence: fabien.picaud@univ-fcomte.fr

8 **Abstract:** Since few years and the achievement of the nanotechnologies, the development of exper-
9 iments based on carbon nanotube has allowed to increase the ionic permeability and/or selectivity
10 in nanodevices. However, this new technology opens the way to a lot of questionable observations,
11 for which theoretical works are able to answer using several approximations. One of these concerns
12 the apparition of a negative charge on the carbon surface, while this latter is apparently neutral.
13 Using first principles functional density theory combined to molecular dynamics, we develop here
14 several simulations on different systems in order to understand the reactivity of the carbon surface
15 in low or ultra-high confinement. Our calculations demonstrate the high affinity of the carbon atom
16 in every situation only for hydrogen ion, and in a less extend, for hydroxyl ion. This latter can only
17 occur when the first hydrogen attack has been achieved. As a consequence, the functionalization of
18 the carbon surface upon the presence of a water media is activated by its protonation, then allowing
19 reactivity of anion.

20 **Keywords:** Quantum simulations, carbon nanotube, graphene, functionalization, confinement.21 **Citation:** Mejri, A.; Herlem, G.;Picaud, F. From behavior of water
on hydrophobic graphene surface to
ultra-confinement of water in carbon
nanotube. *Nanomaterials* **2021**, *11*, x.
<https://doi.org/10.3390/xxxxx>

Received: date

Accepted: date

Published: date

22 **Publisher's Note:** MDPI stays neu-
23 tral with regard to jurisdictional
24 claims in published maps and insti-
25 tutional affiliations.26 **Copyright:** © 2020 by the authors.
27 Submitted for possible open access
28 publication under the terms and
29 conditions of the Creative Commons
30 Attribution (CC BY) license
31 ([http://creativecommons.org/licenses](http://creativecommons.org/licenses/by/4.0/)
32 [by/4.0/](http://creativecommons.org/licenses/by/4.0/)).21 **1. Introduction**

22 Several curved and flat solid structures such as carbon (CNT) [1-6], boron nitrides
23 (BNNT) and silicon carbide [7,8] nanotubes or surfaces [9,10] (graphene [11-16]) are in-
24 teresting candidates for the design of synthetic nanofluidic platforms. The easy control
25 of their diameter during synthesis process can regulate inside liquid flow and transport
26 of charges opening up a wide field of applications in nanomedicine [17-19], biotechnol-
27 ogy, desalination [20-23] membrane nanofiltration [24,25] nanofluidic devices for energy
28 recovery and conversion [26-32] and water filtration [33]. CNTs are able to reproduce
29 the biological properties of their counterparts, but with a less complex composition. For
30 instance, they can notably present a chemical selectivity such as some natural nanochan-
31 nels or transport different species. Many other different properties of bulk fluids could
32 be also observed in such systems due to the surface effect.

33 Simulations and experiments with water confined inside carbon nanotubes can reveal
34 unusual physical properties, especially for diffusion behavior and viscosity. These prop-
35 erties are highly dependent on the geometrical characteristics of the CNT (tube diameter
36 and chirality) and can directly affect water distribution inside the cage leading to unu-
37 sual water performance in confined space [34-40]. Several studies have shown for CNTs
38 and BNNTs an ordered structure of water molecules essentially related to the metallicity
39 and diameter of the tube. Pascal et al. reported that for armchair CNTs with increased
40 diameters, water molecules present a bulk-like behavior when CNTs diameter is above
41 1.4 nm, while an ice-like framework water is characterized for CNTs diameters ranging
42 from 1.1 and 1.2 nm [41]. In a recent theoretical study, molecular dynamic simulations
43

44 reveal that network formation in the form of a water chain-like occurs where molecules
45 are successively arranged in CNT of diameters around 1.1 nm [39], which is in accord-
46 ance with several previous studies [35,42-44]. Shayeganfar et al. reported, thanks to ab
47 initio computations, that a water tube shape is observed when confined in CNTs and
48 BNNTs. They also confirmed that this tendency of water arrangement depends on the
49 diameter for both situations [45].

50 Otherwise, numerous experimental and theoretical studies carried out in recent years
51 have shown that a significant surface charge in both carbon and BN walls occurs in
52 nanofluidic transport systems [9,46]. It has been established that this surface charge can
53 be much higher for BNNT tubes than for CNTs. A plausible explanation for the appear-
54 ance of this surface charge has remained puzzling. But most of the available studies sug-
55 gest that the adsorption of hydroxide ions on hydrophobic surfaces could explain this
56 phenomenon.

57 Sirin et al. have shown in an experimental study that the high surface charge measured
58 on a BNNT connecting two reservoirs could be related to the diameter of the tube as
59 well as to the pH of the studied medium. The hypothesis of a chemical reactivity at the
60 surface of the BNNT has therefore been underlined. Based on previous theoretical stud-
61 ies, it has been proposed that a site of "activated" boron can indeed cause the dissocia-
62 tion of water on the BN sheet [47,48]. Note also that carbon structures could also, both at
63 the theoretical and experimental scales, show a particular ionic selectivity as a function
64 of their diameter and chirality [49,50], which could explain the specific charges of the
65 carbon walls.

66 The good understanding of the mechanism governing the transport of fluid inside car-
67 bon-based materials, at the theoretical scale, would be an essential step in the develop-
68 ment of new generation devices for a wide field of new industrial applications.

69 In fact, simulating the behavior of water molecules towards nanoporous solids is of
70 great interest to investigate promising materials for smart nanofluidic systems under
71 electric bias [51-54]. Consequently, recourse to computational methods would make it
72 possible to establish a realistic approach by reproducing an electrochemical system in
73 which the electrolytes are in contact with a solid polarized surface under the effect of an
74 external uniform electric field [2,55,56].

75 Otani and O. Sugino [57] have developed since 2006 a novel computational scheme
76 which makes it possible to apply an electric bias to the system constituting of a slab as
77 occurring with an electrode and an electrolyte solution. The slab represents a bounded
78 polarized or charged interface between two semi-infinite media having a dielectric con-
79 stant. The method is then called « Effective Screening Medium ». The boundary condi-
80 tions are given to a model unit cell by solving the Poisson equation allowing the creation
81 of an infinite slab.

82 The Effective Screening Medium (ESM) method allows, through the coupling of DFT
83 and molecular dynamics, a rigorous study of electrochemical systems. In the present
84 study, two solid structures were tested against dissociated and undissociated water: the
85 zigzag carbon nanotube and the graphene monolayer. Various quantities were then ex-
86 tracted from this study, in particular the adsorption energy of water on the solid surface,
87 the radial distribution density of the confined water as well as the relevant structural
88 observations.

89 2. Materials and Methods

90 First principles Functional Density theory calculations were used to investigate the
91 interaction of a dissociated and undissociated water molecule with graphene and the car-
92 bon nanotube. The geometry optimization was performed through the « Open source
93 package for Material eXplorer code » (OpenMX) using a combination of molecular dy-
94 namics and local density approximation (LDA) for the exchange-correlation potentials
95 with the Perdew–Burke–Ernzerhof (PBE) functional. Pseudopotentials and wave func-
96 tions have also been implemented to reduce the calculations cost. An investigation of the
97 structural and energetical properties was performed on the studied systems such as ad-
98 sorption energy, ground state geometries of system components, and electronic density
99 of states (DOS). Differences in charge density calculations were also performed by
100 OpenMX code for the adsorption of dissociated water molecules to CNT and graphene
101 structures. This implies a more rigorous understanding of the spin (charges) density re-
102 distribution induced by the interaction of water entities with carbon structures.

103 The total energy scf convergence criterion for the self-consistent electronic minimiza-
104 tion is set at 10^{-6} hartree. Pseudo-atomic orbitals (PAOs) centered on atomic sites were
105 used as basis sets. The basis sets for C, O, Cl, B, N were taken as “s2p2d1”, while those for
106 Na atoms were “s2p2”. The k points are generated according to the Monkhorst-Pack
107 method, and were set to $3 \times 3 \times 1$. The mesh cut-off energy value was set to 170 Ry. Oth-
108 erwise, a large 34 Å vacuum is built into the cell along the z axis to avoid overlapping
109 periodic cells.

110 The adsorption energy (equation 1) is estimated based on a difference between the
111 total energy of the complex tube CNT (and graphene) + adsorbate system and the indi-
112 vidual tube (and graphene) and gas phase free molecule system.

$$113 \text{Eads } H^+/OH^- = E_{\text{tot}}(H^+/OH^-_{\text{ads_surface}}) - E(H^+/OH^-_{\text{des_surface}}) \quad (1)$$

114
115 For all the simulations, molecular dynamics calculations were carried out in the
116 NVT_VS ensemble at 300 K. The velocities of the atoms were scaled every 20 MD steps
117 and time step is of 1 fs. All simulations were run for 2000 fs.

118 Monolayer graphene is made of 32 atoms and adopts an armchair chirality (1,1) with
119 honeycomb structure. and semi-metallic properties. The monolayers of each system are
120 separated by a 34 Å vacuum to avoid any interaction between the periodic images.

121 Carbon nanotubes have been also studied with a confined water molecule and the
122 same vacuum exclusive region as previously. For all the structures, two situations are in-
123 vestigated: a first case with an undissociated water molecule and a second one with a
124 dissociated water molecule. In each situation, the cases without field and with field appli-
125 cation are also explored.

126 3. Results

127 3.1. Water molecule interaction with graphene walls

128 Graphene has become a key component in the development of graphitic nanoslits for
129 the transport of water and ion [58-60]. But there is still an important lack in the theoretical
130 studies which analyze the behavior of water towards this material since many experi-
131 mental observations are still interpreted as coming from the apparition of a surface charge.
132 The origin of this latter needs a more profound theoretical insight to understand its ap-
133 pearance. Hence, it seemed relevant to investigate more closely the behavior of a dissoci-
134 ated water molecule near a single graphene sheet. An uniform electric field is applied to
135 the system to model the influence of the potential drop used in current-voltage measure-
136 ments. Figure 1 shows the system studied, and summarizes the ESM method model used
137 in these calculations.

138 The same calculations were also performed for an undissociated water molecule, the
139 applied field did not cause the spontaneous dissociation of the water molecule even for
140 high intensities.
141

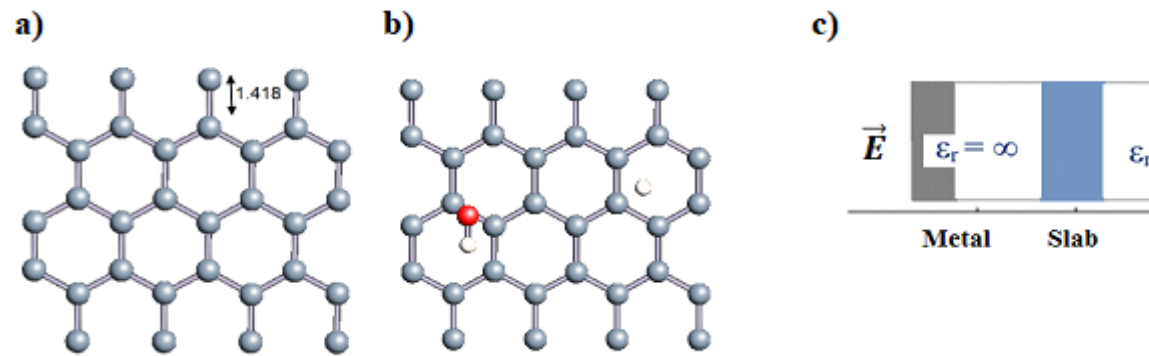


Figure 1. a, b) Graphene and dissociated water + graphene system. c) ESM method model.

As shown in Table 1, which summarizes all the adsorption energies of H⁺ and OH⁻ on the graphene surface due to the most important events occurring during the simulation, the adsorption states of H⁺ and HO⁻ are all negative indicating favorable adsorption in each case. The first adsorption energy of each entity is called E_{ads}. H⁺ and E_{ads} HO⁻.

In the three 2000 fs simulations, the adsorption of the H⁺ is noted at fast times. For fields equal to 0 eV and -5 eV, HO⁻ adsorption was not observed. A very high field intensity, only, lets the adsorption of HO⁻ occurs.

Table 1. Adsorption states and energies of dissociated water molecule on graphene monolayer.

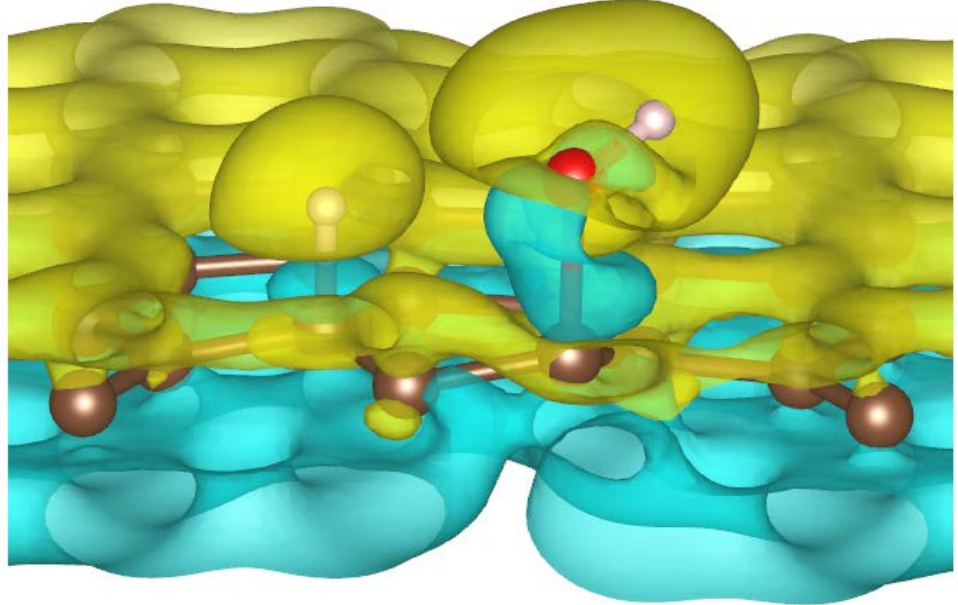
U(eV)	0	-5	-50
Figure			
Observation	H ⁺ adsorption at 79 fs H ₂ O formation at 365 fs.	H ⁺ adsorption at 63 fs H ₂ O formation at 365 fs	H ⁺ adsorption at 40 fs HO ⁻ adsorption at 906 fs
E _{ads} . H ⁺ (eV)	-0.9	-1.3	-1.5
E _{ads} . HO ⁻ (eV)	-	-	-0.6

The hydrogen adsorption energies are in agreement with the theoretical calculations observed in the literature which ranged from -0.81 [61] for the PBE method to -0.67 in LSDA [62].

The adsorption energy of HO⁻ is not favored in the first two situations, when the electric field value is of low intensity. It can only occur with a strong field but presents a value which remains in agreement with the literature for this type of systems. Note that the adsorption of HO⁻ is only possible after a first adsorption of H⁺ thus creating a defect in the electronic structure of the planar surface. This has been already observed in recent

168 data since the HO- adsorption on graphene was never chemical and lead to small interac-
 169 tion energies with carbon atom.

170 To better understand the ability of the hydrogen or hydroxyl ions to interact with the
 171 graphene sheet, we represent in Figure 2, the charge density distribution differences for
 172 dissociated water molecule near graphene sheet.



173 **Figure 2.** Charge-density distribution in case of dissociated water molecule adsorp-
 174 tion on graphene at -50 eV electric field. Yellow and blue lobes represent respectively the
 175 positively and negatively charged areas.
 176

177
 178 As shown in Figure 2, the surface polarization generated by the effect of the electric
 179 field creates negative and positive charges on the carbon atoms of the graphene. This po-
 180 larization allows H⁺ ion to be adsorbed on the carbon atoms which presents a negative
 181 surface layer. Indeed, H⁺ is forced to translate in the field direction, as the partial charges
 182 on the graphene surface do. This induces favorable adsorption of H⁺ at the first step of
 183 the simulation. Once H⁺ is linked to a carbon atom, it modifies locally the density of
 184 charge repartition. Without such changes, HO- could never be adsorbed on the graphene
 185 surface. The presence of the cation allows thus to HO- to be attracted by the graphene sur-
 186 face spontaneously.

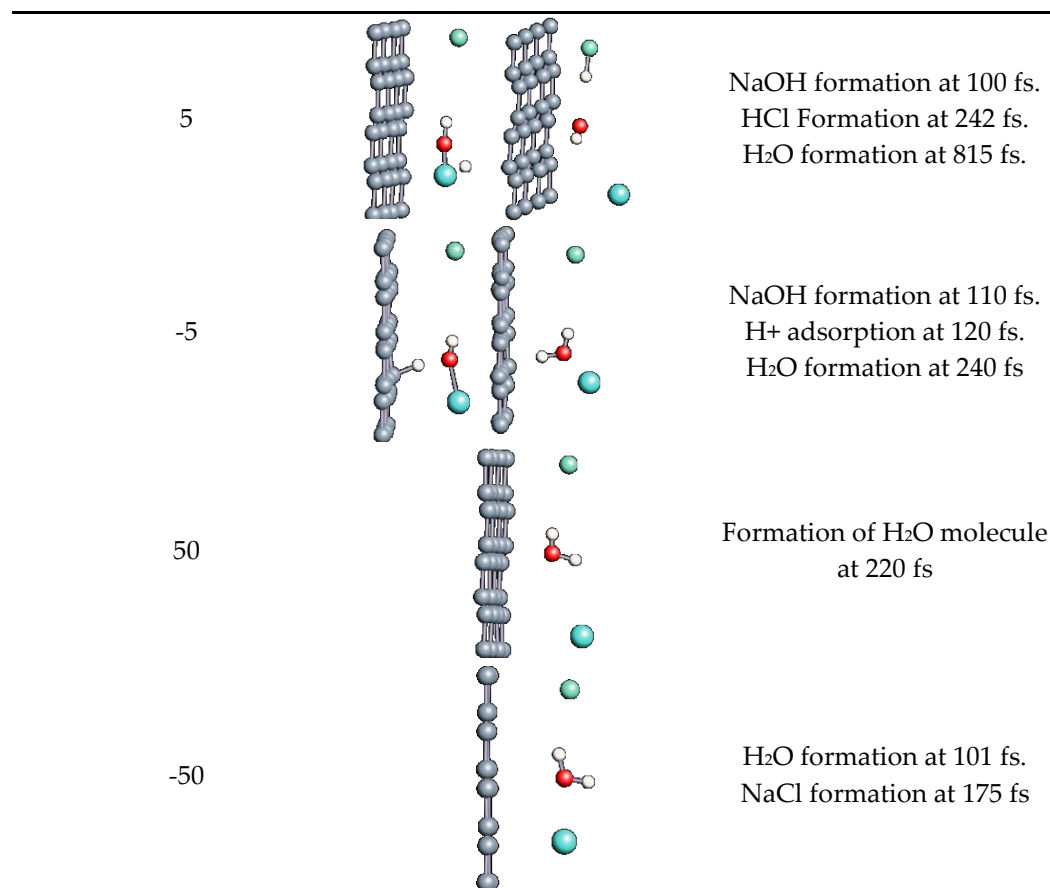
187 3.1.1. Salt effect

188 The role of salt in the water dynamic is necessary to complete the simulated system
 189 and to approximate the experimental conditions. The dissociated sodium chloride (Na⁺,
 190 Cl⁻) has thus been added to the previous system.

191 The behavior of water and salt with respect to graphene at different field strengths is
 192 given in Table 2.

193
 194 **Table 2.** Behavior of dissociated water molecule near graphene layer in the presence
 195 of salt under electric bias

U(eV)	Important events in simula- tion	Observations
0		H ⁺ adsorption at 135 fs. H ₂ O formation at 292 fs.



196
197
198
199
200
201
202
203
204
205
In all the simulations, the reformation of water molecules from H⁺ and HO⁻ in solution is observed at relatively short times for all field intensities. However, for weak field intensities, short-lived interactions of H⁺ with the carbon surface are possible but are not really relevant. There is no a real OH⁻ and H⁺ adsorption phenomenon on the graphene surface in the presence of salt in these simulations. Note that during the simulations, the reformation of NaCl is observed close to the graphene surface in our electrochemical ESM cell. There is thus no possibility for salt ions to be kept by the graphene surface.

3.2. Undissociated water molecule inside the carbon nanotube

206
207
208
209
210
211
212
213
214
215
216
217
218
219
220
The role of the confinement at the nanometric scale on the possibility to charge a carbon wall was then studied. Indeed, it has been established in previous experimental and theoretical studies [63-65] that the water dissociation can occur under the effect of an electric field. Furthermore, studies of the water behavior in an ultra-confined environment have not excluded the possibility of its dissociation [66,67]. This dissociation can be very favored in a confined space, in fact, Muñoz-Santiburcio et al. have shown that confinement greatly improves the self-dissociation process of water. This result is consistent with another study conducted by Sirkin et al. who used QM/MM molecular dynamics to compute the energy without water dissociation in a single-walled carbon nanotube 8.1 Å diameter. They hypothesized that it seems plausible, under the effect of nanometric confinement, to see an increase in the self-dissociation constant due to the increase in the permittivity of the confined fluid [67]. We first modeled a (16,0) single-walled carbon nanotube with diameter equal to 1.35 nm where a water molecule is introduced in the confined inner space of the carbon cage. Several situations have been achieved by increasing the field intensity (Fig. 3).

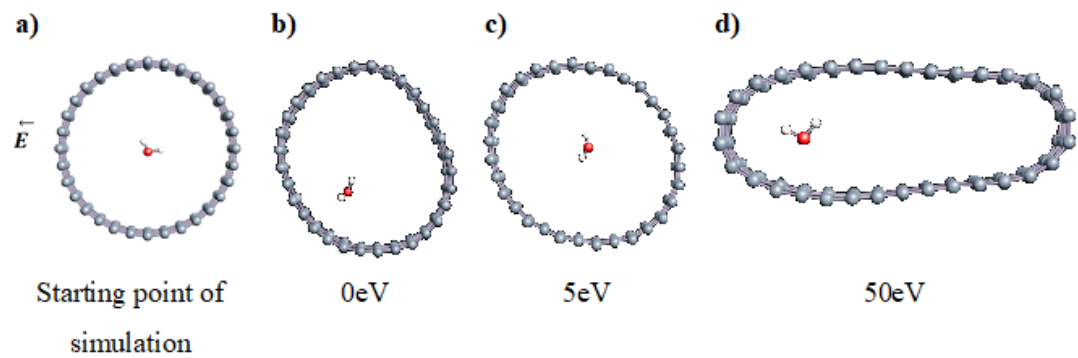


Figure 3. electrical polarization effect on water@tube system.

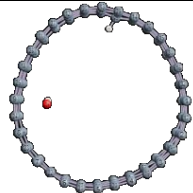
Despite the importance of the applied field intensities which strongly impact the geometry of the carbon nanotube, we did never observe any dissociation of confined water molecule. There is a deformation of the nanotube until it becomes crushed and takes an elongated shape in the transverse direction (Fig. 3d). Whatever the deformation, the molecule diffuses inside the inner volume of the CNT, exploring different atomic positions but keeping its distance from carbon wall due to hydrophobic interaction.[68] Note that no form of physical or chemical adsorption of the water molecule is noted on the carbon surface.

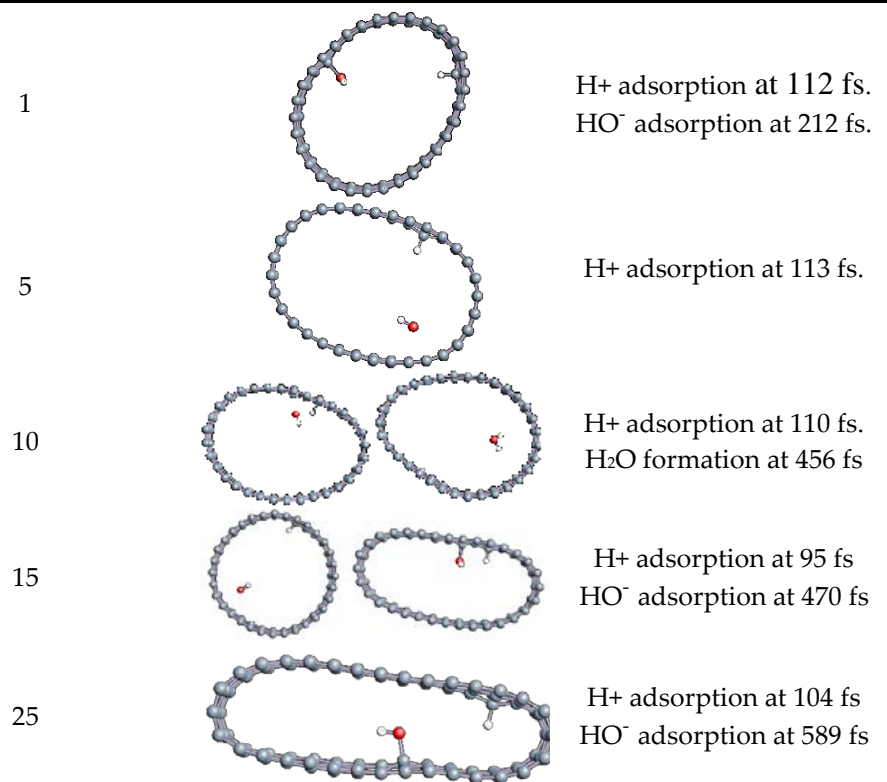
3.2.1. Dissociated water molecule inside CNT

Since no dissociation of the molecule was achieved under the action of an electric field or not in our previous modelization, the next step of our calculations deals with the simulation of a dissociated water molecule inside the carbon cage. In this case, we study directly the possibility of hydronium and hydroxyl ions adsorption resulting from this dissociation and quantify it in terms of adsorption energy. Several simulations were undertaken for a dissociated water molecule confined inside the carbon nanotube (16,0). The main results are shown in Table 3 and 4.

We first noted that the H^+ adsorption is possible spontaneously without any external contribution of an electric field as seen for the first simulation at 0 eV field intensity. In addition, our calculations show that the adsorption of H^+ always precedes that of HO^- regardless the intensity of the applied field. Note here that the hydrogen adsorption is favored rapidly and did not depend on the deformation of the carbon cage under the electric field intensity. The rapid process leading to the hydrogenation of a carbon has been observed before the strong modification of the carbon geometry. On the contrary, the formation of water molecule (observed for $E=10\text{eV}$) or the adsorption of hydroxyl is only possible when H^+ is chemisorbed and carbon surface is deformed under increasing electric field intensity, as observed previously.

Table 3. water molecule dissociated inside (16,0) CNT under electric bias.

U(eV)	Important events in simulation	Observations
0		H^+ adsorption at 140 fs.



The last two simulations gathered in Table 3 (performed at 15 eV and 25 eV) recall the case of graphene for a dissociated water molecule. In fact, HO⁻ adsorption takes place at later times in the simulation but especially at high field intensities and for an important carbon deformation. We reported in Table 4 the different adsorption energies obtained when hydrogen and/or hydroxyl ions are adsorbed on the carbon wall.

Table 4. (H⁺, HO⁻) Adsorption energies inside (16,0) CNT

U(eV)	H ⁺ Ads. energy (eV)	HO ⁻ ads. energy (eV)
0	-4.1	-
1	-4.2	-0.3
5	-4.0	-
10	-4.6	-
15	-4.6	-0.06
20	-4.3	-
25	-4.2	-0.3

The energies calculated for H⁺ adsorption in the inner surface of the carbon cage are of the order of -4 eV. These clearly show that the adsorptions observed are chemisorptions, explaining the difficult for hydroxyl ion to interact with hydrogen once chemisorbed. These values remain in agreement with other found in the literature which ranged around -3eV [69]. Note also that for each modification of the carbon surface by the hydrogen chemisorption, we observed a modification of the carbon hybridation which could be apparent to a sp³ mode. The hydroxyl ion interacted with the carbon surface with a higher energy, which remains comparable with those obtained in the literature. [70]

3.2.2 Differences in charge density distribution for the dissociated water molecule inside CNT

In figure 4, we plot the modification of the atomic charge density with time upon the application of high electric field intensity (25eV). The positive and negative differences in total charge densities are colored in yellow and blue, respectively. As seen in Fig. 4, the polarization of the surface is responsible for the delocalization of electrons and therefore for the creation of an electron deficit on certain areas of the internal surface of the tube and an accumulation of electrons in other areas. As a consequence, the hydrogen ion will be more sensitive to the surface zone where the electrons are present while the hydroxyl remains close to surface part charged in an opposite way. However, even in this large field intensity, the time necessary to obtain the hydroxyl binding to the carbon surface is quite large (627 fs) while hydrogen ion is attached faster to the surface (85 fs compared to 110 fs at least).

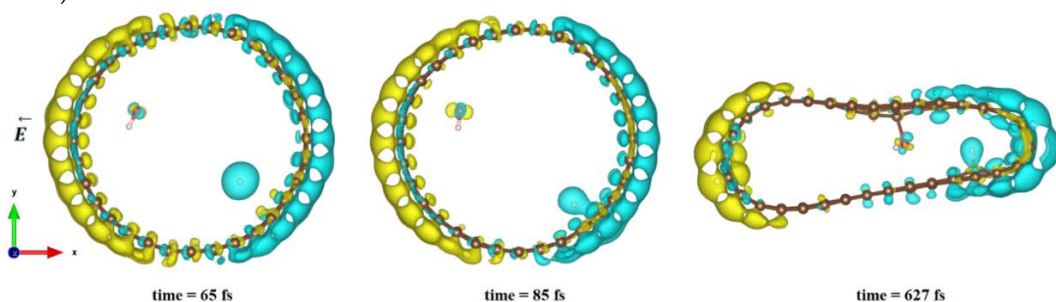


Figure 4. Difference in charge density distribution of the dissociated water molecule inside the CNT under 25 eV electric field. The yellow and blue lobes represent the positively and negatively charged areas, respectively.

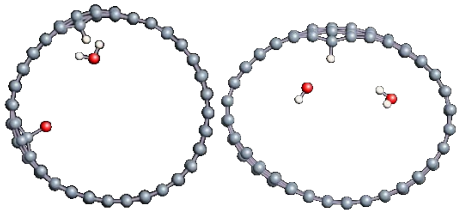
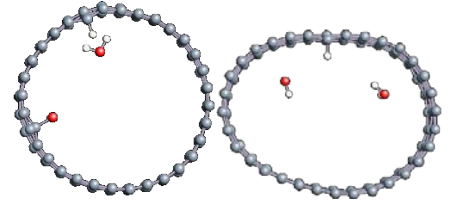
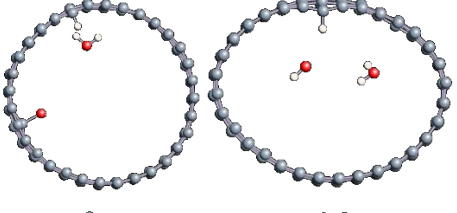
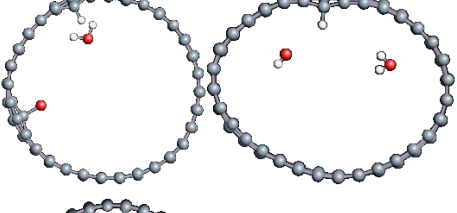
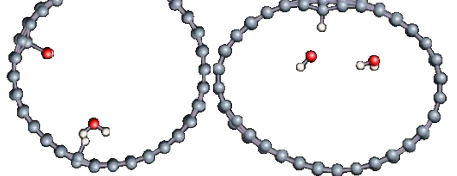
3.2.3. Effect of adding water molecules on the adsorption steps

To go further in our study, we complicated the previous system by adding an additional water molecule and let the system evolve to see its effect on the adsorption steps. Several simulations were performed by varying the intensity of the applied field. A domain of intensities ranging from 0 to 30 eV was scanned. Table 5 illustrates all the simulations carried out for this system containing one dissociated and one undissociated water molecule inside the carbon nanotube (16,0).

As shown in Table 5, the same behavior is almost detected in all the simulations, even at high field strengths. The phenomena of H⁺ and HO⁻ adsorption occurs at practically simultaneous instants with a very slight advance of HO⁻ adsorption of a few fs over the H⁺ adsorption, compared to the previous system. This first HO⁻ adsorption, before any other, is the main difference obtained in this system which has never been observed previously. However, it is not very durable because the entity is desorbed in all cases after 40 fs of existence, depicting a very low adsorption energy with carbon atom. On the other hand, H⁺ remains adsorbed until the end of the simulation in all situations, as observed previously. We may thus question on the role of HO⁻ on the H⁺ adsorption in this case. It can either be the main factor which improved the association of hydrogen with carbon by the modification of the electronic structure of the cage or, simply, be the random consequence of the hydroxyl position compared to the hydrogen position. Note that no dissociation of the water molecule has been observed during the simulation.

Table 5. Dissociated and undissociated water molecules inside (16,0) CNT under electric bias

308

Field intensity (eV)	Important events	Observation
1		134 fs HO ⁻ adsorb 150 H ⁺ 179 HO ⁻ desorption
10		135 HO ⁻ 137 H ⁺ 173 HO ⁻ desorption
15		133 HO ⁻ 137 H ⁺ 167 HO ⁻ desorption
20		133 HO ⁻ 138 H ⁺ 173 HO ⁻ desorption
30		133 HO ⁻ 136 H ⁺ 177 HO ⁻ desorption

309

310

311

312

313

314

315

316

Adsorption energies were calculated. Results are reported in Table 6. Due to very fast hydroxyl adsorption events, we were not able to estimate precisely the adsorption energy for HO⁻ ion. However, as seen in Table 6, the hydrogen adsorption energy remains equal to -4.4 eV as obtained previously (Table 4) for the system where no water molecule was present in the system. The role of the water molecule added to the hydrogen plus hydroxyl ion seems to play a minor role in the reactivity of the carbon surface.

Table 6. H⁺ Adsorption energies inside (16,0) CNT

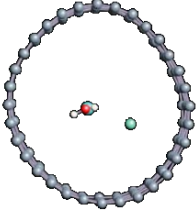
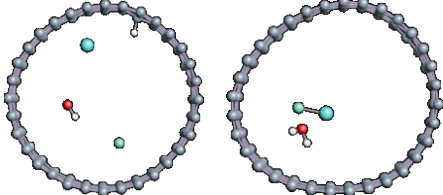
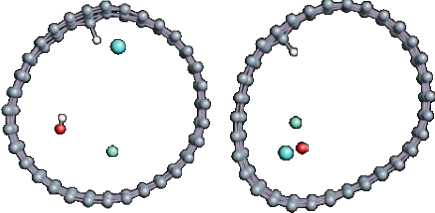
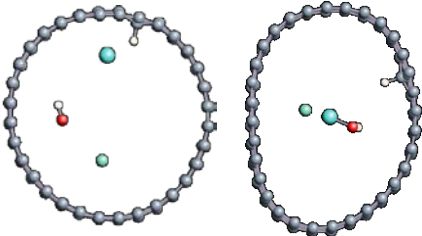
U(eV)	H ⁺ Ads. energy (eV)
1	-4.413
10	-4.408
15	-4.426
20	-4.409
30	-4.508

317
 318
 319
 320
 321
 322
 323
 324
 325
 326
 327
 328
 329
 330

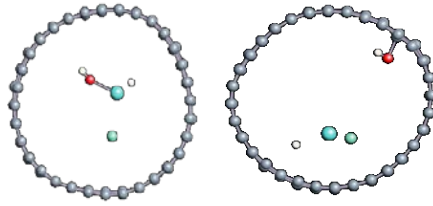
3.2.4. Salt effect on adsorption phenomena

In order to evaluate the effect of ions on the adsorption of dissociated water inside carbon nanotube, we added to the dissociated H₂O @ CNT system, a salt composed of a unique Na⁺ ion and its counterion Cl⁻. The different adsorption events as a function of the increasing field intensity are summarized in Table 7. For intensities between 5 and 20 eV, H⁺ adsorption first occurs at around 80 fs followed by the rapid reformation of the water molecule. At a field of 25 eV, HO⁻ adsorption occurs first, at about 385 fs and the entity remains adsorbed for 200 fs. Note that CNT is much less deformed under the action of an intense electric field when it contains more molecules and that no dissociation of water molecule is observed once formed.

Table 7. Dissociated water molecules inside (16,0) CNT under electric bias in presence of a salt.

Field Intensity (eV)	Important events in simulation	Observations
0		H ₂ O is formed at 250 fs
5		H ⁺ adsorbed at 75 fs H ₂ O is formed at 551 fs
10		H ⁺ is adsorbed at 90 fs and HO ⁻ remains free until the end of the simulation
20		H ⁺ is adsorbed at 83 fs and HO ⁻ remains free until the end of the simulation. NaOH formation.

25



NaOH formation at 268 fs.

HO⁻ adsorption at 385 fs.HO⁻ desorption at 556 fs.331
332
333
334
335
336
337

As for other systems, we estimate the H⁺ and HO⁻ adsorption energies in Table 8. We observe that the adsorption of H⁺ is less favorable in this case (-4 eV at best) while the adsorption of HO⁻ in the very high electric field intensity is of the same order than the H⁺ one. The rapid desorption of HO⁻ cannot explain this result but the presence of Na⁺ allows it. Indeed, we observe an important role played by the salt which are alternatively attracted by either hydrogen or hydroxyl ions in order to form another strong acid or base component.

338

Table 8. H⁺ Adsorption energies inside (16,0) CNT in presence of salt

U(eV)	H ⁺ Ads. energy (eV)	H ⁺ Ads. duration (fs)	HO ⁻ ads. energy (eV)	HO ⁻ ads. duration (fs)
0	-	-	-	-
5	-3.288	476	-	-
10	-3.449	1910	-	-
20	-4.087	1917	-	-
25	-	-	-3.211	171

339
340
341
342
343
344
345

3.2.5. Several water molecules inside (16,0) carbon nanotube

In order to get closer to biological conditions, a system with dissociated water molecule submersed in several water molecules is simulated by varying the intensity of the applied electric field. The density of water has been calculated to 1 in order to reproduce a bulk like water media. After 2000 fs simulations we observe in all cases a rapid formation of water molecule (in 17 fs).

346

Table 9. distribution of water inside the (16,0) carbon nanotube

Field intensity (Ev)	0	10	25	50
Water distribution				
First maximum position (Å)	2.66	2.73	2.75	2.75

347
348
349

In order to check the conformation of the confined water and to see if possibly a phase change has taken place, we calculated the radial distribution density of the water in the various studied situations. The calculated values are entered as the water at the end of the

simulation keeps the structure of the liquid phase and summarized in Table 10. For each case, the first peak is localized at nearly 2.7 Å. This value corroborates the organization of the water molecule as a liquid since the experimental value for liquid water which is 2.88 Å.

Table 10. First peak position in the radial distribution function of confined water.

U(eV)	First maximum position (Å)
0	2.658
10	2.73
25	2.754
50	2.75

Experimental Value for liquid water $\rho_{OO1} = 2.88$

Note that during the simulation, while no adsorption was observed on the carbon surface, the formation of successive hydronium ion inside the water bulk and proton jump have been effective via the so-called Grotthuss mechanism.

3.3. Change in hybridization of the adsorption site

We found by comparing the two carbon structures that the adsorption of HO⁻ on carbon nanotubes is much more favorable than on graphene monolayer and takes place at lower field intensities. This is probably due to the higher surface charge of the carbon nanotube and its coiled structure.

We noted here for the carbon structures, that a change of conformation is observed for the carbon atom at the adsorption site (see figure 5). Indeed, as established by previous studies, the adsorption of an entity on a graphene surface or on the internal or external surface of a single-walled carbon nanotube modified the adsorption site initially hybridized sp² (planar structure). Due to the adsorption it deviates from its original state towards sp³ type hybridization. It is then the center of a regular tetrahedron defined by three adjacent carbon atoms and the adsorbed entity. This strong local deformation causes a change in the bond angles of the original sp² hybridization (CCC) = 120° to (CCC) = 112° respectively for CNT and graphene.

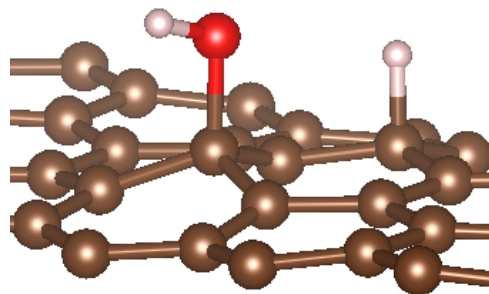


Figure 5. sp³ hybridization of the adsorption site for graphene material.

Note also that the observed bond lengths are C-Hgraphene = 1.1 Å; C-HCNT = 1.12 Å; C-Ographene = 1.52; C-OCNT = 1.496 Å, which are very characteristic of single bonds for each of the studied structures. The puckering of the carbon atom beneath the adsorbed

hydrogen atom, leads to an increase in its sp^3 character [9,13,15,69,71-76]. A stretching in the C–C bonds associated with this carbon atom is also noted. They are approximately 0.3 Å elongated from the original C–C bond length in pure structures. Casolo et al. quantified the electronic rearrangement of the carbon atom by a high energy barrier of 0.2 eV [71,77].

5. Conclusions

In this work, we studied through DFT-MD calculations the analysis of flat (graphene) or curved (CNT) carbon surface reactivities to proton and hydroxyl ions or hydroxyl ions, mixed or not with other entities, upon the presence of an electric field or not at the molecular scale. From all of our studies, we demonstrated here a very strong affinity of the carbon wall, whatever its curvature, for proton, with a notable modification of the hybridization of carbon atom. The adsorption energy obtained in each case is about -4eV, in agreement with literature. On the contrary, we can note that no specific adsorption preferences have been characterized for HO⁻ ion. Some punctual observations of hydroxyl interaction with the carbon surface have been obtained, but mainly after a first functionalization of the carbon by the hydrogen in the presence and absence of an electric field. However, the higher the electric field intensity, the faster the proton chemisorption rate. For graphene, the presence of a dissociated salt (NaCl) with water lead to desorption of ions, while HO⁻ can adsorb first as observed in CNT charged with NaCl. This asymmetry of ion adsorptions occurs on flat and curved carbonaceous surfaces but can be drastically affected by an external electric field, while being pH dependent in water.

Author Contributions: “Conceptualization and methodology, A.M., G.H. and F.P.; simulation, A.M.; writing—original draft preparation, A.M.; writing—review G.H. and F. P. and editing, F.P. All authors have read and agreed to the published version of the manuscript.”

Acknowledgments: This work was funded by Agence Nationale de la Recherche (ANR-18-CE09-0011-01 “IONESCO”). Single tracks have been produced in GANIL (Caen, France) in the framework of an EMIR project. Calculations were performed at the supercomputer regional facility Mesocentre of the University of Franche-Comté with the assistance of K. Mazouzi. This work was also granted access to the HPC resources of IDRIS, Jean Zay supercomputer, under the allocation 2019 - DARI A0070711074 made by GENCI. Finally, part of this work was performed using computing resources of CRIANN (Normandy, France).

Conflicts of Interest: “The authors declare no conflict of interest.”

References

1. Vaitheeswaran, S.; Rasaiah, J.C.; Hummer, G. Electric field and temperature effects on water in the narrow nonpolar pores of carbon nanotubes. *The Journal of Chemical Physics* **2004**, *121*, 7955-7965, doi:10.1063/1.1796271.
2. Mikami, F.; Matsuda, K.; Kataura, H.; Maniwa, Y. Dielectric Properties of Water inside Single-Walled Carbon Nanotubes. *ACS Nano* **2009**, *3*, 1279-1287, doi:10.1021/nn900221t.
3. Kyakuno, H.; Fukasawa, M.; Ichimura, R.; Matsuda, K.; Nakai, Y.; Miyata, Y.; Saito, T.; Maniwa, Y. Diameter-dependent hydrophobicity in carbon nanotubes. *The Journal of Chemical Physics* **2016**, *145*, 064514, doi:10.1063/1.4960609.
4. Hassan, J.; Diamantopoulos, G.; Homouz, D.; Papavassiliou, G. Water inside carbon nanotubes: structure and dynamics. *Nanotechnology Reviews* **2016**, *5*, 341, doi:https://doi.org/10.1515/ntrev-2015-0048.

- 422 5. Yao, Y.-C.; Taqieddin, A.; Alibakhshi, M.A.; Wanunu, M.; Aluru, N.R.; Noy, A. Strong Electroosmotic Coupling
423 Dominates Ion Conductance of 1.5 nm Diameter Carbon Nanotube Porins. *ACS Nano* **2019**, *13*, 12851-12859,
424 doi:10.1021/acsnano.9b05118.
- 425 6. Thiruraman, J.P.; Masih Das, P.; Drndić, M. Ions and Water Dancing through Atom-Scale Holes: A Perspective
426 toward "Size Zero". *ACS Nano* **2020**, *14*, 3736-3746, doi:10.1021/acsnano.0c01625.
- 427 7. Khademi, M.; Sahimi, M. Molecular dynamics simulation of pressure-driven water flow in silicon-carbide
428 nanotubes. *The Journal of Chemical Physics* **2011**, *135*, 204509, doi:10.1063/1.3663620.
- 429 8. Barghi, S.H.; Tsotsis, T.T.; Sahimi, M. Hydrogen sorption hysteresis and superior storage capacity of silicon-
430 carbide nanotubes over their carbon counterparts. *International Journal of Hydrogen Energy* **2014**, *39*,
431 21107-21115, doi:https://doi.org/10.1016/j.ijhydene.2014.10.087.
- 432 9. Grosjean, B.; Pean, C.; Siria, A.; Bocquet, L.; Vuilleumier, R.; Bocquet, M.-L. Chemisorption of Hydroxide on
433 2D Materials from DFT Calculations: Graphene versus Hexagonal Boron Nitride. *The Journal of Physical*
434 *Chemistry Letters* **2016**, *7*, 4695-4700, doi:10.1021/acs.jpcllett.6b02248.
- 435 10. Comtet, J.; Grosjean, B.; Glushkov, E.; Avsar, A.; Watanabe, K.; Taniguchi, T.; Vuilleumier, R.; Bocquet, M.-L.;
436 Radenovic, A. Direct observation of water-mediated single-proton transport between hBN surface defects.
437 *Nature Nanotechnology* **2020**, *15*, 598-604, doi:10.1038/s41565-020-0695-4.
- 438 11. Striolo, A.; Chialvo, A.A.; Cummings, P.T.; Gubbins, K.E. Water Adsorption in Carbon-Slit Nanopores.
439 *Langmuir* **2003**, *19*, 8583-8591, doi:10.1021/la0347354.
- 440 12. Cole, D.J.; Ang, P.K.; Loh, K.P. Ion Adsorption at the Graphene/Electrolyte Interface. *The Journal of Physical*
441 *Chemistry Letters* **2011**, *2*, 1799-1803, doi:10.1021/jz200765z.
- 442 13. Wang, Y.; Qian, H.-J.; Morokuma, K.; Irlle, S. Coupled Cluster and Density Functional Theory Calculations of
443 Atomic Hydrogen Chemisorption on Pyrene and Coronene as Model Systems for Graphene Hydrogenation.
444 *The Journal of Physical Chemistry A* **2012**, *116*, 7154-7160, doi:10.1021/jp3023666.
- 445 14. Park, H.G.; Jung, Y. Carbon nanofluidics of rapid water transport for energy applications. *Chemical Society*
446 *Reviews* **2014**, *43*, 565-576, doi:10.1039/C3CS60253B.
- 447 15. Chawla, J.; Kumar, R.; Kaur, I. Carbon nanotubes and graphenes as adsorbents for adsorption of lead ions
448 from water: a review. *Journal of Water Supply: Research and Technology-Aqua* **2015**, *64*, 641-659,
449 doi:10.2166/aqua.2015.102.
- 450 16. Xie, Q.; Alibakhshi, M.A.; Jiao, S.; Xu, Z.; Hempel, M.; Kong, J.; Park, H.G.; Duan, C. Fast water transport in
451 graphene nanofluidic channels. *Nature Nanotechnology* **2018**, *13*, 238-245, doi:10.1038/s41565-017-0031-9.
- 452 17. Gao, W.; Kong, L.; Hodgson, P. Atomic interaction of functionalized carbon nanotube-based nanofluids with a
453 heating surface and its effect on heat transfer. *International Journal of Heat and Mass Transfer* **2012**, *55*,
454 5007-5015, doi:https://doi.org/10.1016/j.ijheatmasstransfer.2012.04.044.
- 455 18. Goenka, S.; Sant, V.; Sant, S. Graphene-based nanomaterials for drug delivery and tissue engineering. *Journal*
456 *of controlled release : official journal of the Controlled Release Society* **2014**, *173*, 75-88,
457 doi:10.1016/j.jconrel.2013.10.017.
- 458 19. Mejri, A.; Delphine, V.; Tangour, B.; Gharbi, T.; Picaud, F. Encapsulation Into Carbon Nanotubes and Release
459 of Anticancer Cisplatin Drug Molecule. *The journal of physical chemistry. B* **2014**, *119*,
460 doi:10.1021/jp5102384.
- 461 20. Corry, B. Designing Carbon Nanotube Membranes for Efficient Water Desalination. *The Journal of Physical*
462 *Chemistry B* **2008**, *112*, 1427-1434, doi:10.1021/jp709845u.

- 463 21. Dai, H.; Xu, Z.; Yang, X. Water Permeation and Ion Rejection in Layer-by-Layer Stacked Graphene Oxide
464 Nanochannels: A Molecular Dynamics Simulation. *The Journal of Physical Chemistry C* **2016**, *120*, 22585-
465 22596, doi:10.1021/acs.jpcc.6b05337.
- 466 22. Suss, M.E.; Porada, S.; Sun, X.; Biesheuvel, P.M.; Yoon, J.; Presser, V. Water desalination via capacitive
467 deionization: what is it and what can we expect from it? *Energy & Environmental Science* **2015**, *8*, 2296-
468 2319, doi:10.1039/C5EE00519A.
- 469 23. Wang, X.; Shi, G.; Liang, S.; Liu, J.; Li, D.; Fang, G.; Liu, R.; Yan, L.; Fang, H. Unexpectedly High Salt
470 Accumulation inside Carbon Nanotubes Soaked in Dilute Salt Solutions. *Physical Review Letters* **2018**, *121*,
471 226102, doi:10.1103/PhysRevLett.121.226102.
- 472 24. Williams, C.D.; Carbone, P. Selective Removal of Technetium from Water Using Graphene Oxide Membranes.
473 *Environmental Science & Technology* **2016**, *50*, 3875-3881, doi:10.1021/acs.est.5b06032.
- 474 25. Musielak, M.; Gagor, A.; Zawisza, B.; Talik, E.; Sitko, R. Graphene Oxide/Carbon Nanotube Membranes for
475 Highly Efficient Removal of Metal Ions from Water. *ACS Applied Materials & Interfaces* **2019**, *11*, 28582-
476 28590, doi:10.1021/acsami.9b11214.
- 477 26. Pumera, M. Graphene-based nanomaterials for energy storage. *Energy Environ. Sci.* **2011**, *4*, 668-674,
478 doi:10.1039/C0EE00295J.
- 479 27. Zhai, Y.; Dou, Y.; Zhao, D.; Fulvio, P.F.; Mayes, R.T.; Dai, S. Carbon Materials for Chemical Capacitive Energy
480 Storage. *Advanced Materials* **2011**, *23*, 4828-4850, doi:10.1002/adma.201100984.
- 481 28. Simon, P.; Gogotsi, Y. Capacitive Energy Storage in Nanostructured Carbon–Electrolyte Systems. *Accounts of*
482 *Chemical Research* **2013**, *46*, 1094-1103, doi:10.1021/ar200306b.
- 483 29. Ye, J.; Simon, P.; Zhu, Y. Designing ionic channels in novel carbons for electrochemical energy storage.
484 *National Science Review* **2019**, *7*, 191-201, doi:10.1093/nsr/nwz140.
- 485 30. Xiao, K.; Jiang, L.; Antonietti, M. Ion Transport in Nanofluidic Devices for Energy Harvesting. *Joule* **2019**, *3*,
486 2364-2380, doi:10.1016/j.joule.2019.09.005.
- 487 31. Feng, Y.; Zhu, W.; Guo, W.; Jiang, L. Bioinspired Energy Conversion in Nanofluidics: A Paradigm of Material
488 Evolution. *Advanced Materials* **2017**, *29*, 1702773, doi:10.1002/adma.201702773.
- 489 32. Daiguji, H.; Yang, P.; Szeri, A.J.; Majumdar, A. Electrochemomechanical Energy Conversion in Nanofluidic
490 Channels. *Nano Letters* **2004**, *4*, 2315-2321, doi:10.1021/nl0489945.
- 491 33. Hawks, S.A.; Cerón, M.R.; Oyarzun, D.I.; Pham, T.A.; Zhan, C.; Loeb, C.K.; Mew, D.; Deinhart, A.; Wood, B.C.;
492 Santiago, J.G., et al. Using Ultramicroporous Carbon for the Selective Removal of Nitrate with Capacitive
493 Deionization. *Environmental Science & Technology* **2019**, *53*, 10863-10870, doi:10.1021/acs.est.9b01374.
- 494 34. Köhler, M.H.; da Silva, L.B. Size effects and the role of density on the viscosity of water confined in carbon
495 nanotubes. *Chemical Physics Letters* **2016**, *645*, 38-41, doi:https://doi.org/10.1016/j.cplett.2015.12.020.
- 496 35. Agrawal, K.V.; Shimizu, S.; Drahusuk, L.W.; Kilcoyne, D.; Strano, M.S. Observation of extreme phase
497 transition temperatures of water confined inside isolated carbon nanotubes. *Nature Nanotechnology* **2017**,
498 *12*, 267-273, doi:10.1038/nnano.2016.254.
- 499 36. Fumagalli, L.; Esfandiar, A.; Fabregas, R.; Hu, S.; Ares, P.; Janardanan, A.; Yang, Q.; Radha, B.; Taniguchi, T.;
500 Watanabe, K., et al. Anomalously low dielectric constant of confined water. *Science* **2018**, *360*, 1339-1342,
501 doi:10.1126/science.aat4191.
- 502 37. Zaragoza, A.; Gonzalez, M.A.; Joly, L.; López-Montero, I.; Canales, M.A.; Benavides, A.L.; Valeriani, C.
503 Molecular dynamics study of nanoconfined TIP4P/2005 water: how confinement and temperature affect

- diffusion and viscosity. *Physical Chemistry Chemical Physics* **2019**, *21*, 13653-13667, doi:10.1039/C9CP02485A.
38. de Freitas, D.N.; Mendonça, B.H.S.; Köhler, M.H.; Barbosa, M.C.; Matos, M.J.S.; Batista, R.J.C.; de Oliveira, A.B. Water diffusion in carbon nanotubes under directional electric fields: Coupling between mobility and hydrogen bonding. *Chemical Physics* **2020**, *537*, 110849, doi:https://doi.org/10.1016/j.chemphys.2020.110849.
39. Velioglu, S.; Karahan, H.E.; Goh, K.; Bae, T.-H.; Chen, Y.; Chew, J.W. Metallicity-Dependent Ultrafast Water Transport in Carbon Nanotubes. *Small* **2020**, *16*, 1907575, doi:10.1002/smll.201907575.
40. Barati Farimani, A.; Aluru, N.R. Spatial Diffusion of Water in Carbon Nanotubes: From Fickian to Ballistic Motion. *The Journal of Physical Chemistry B* **2011**, *115*, 12145-12149, doi:10.1021/jp205877b.
41. Pascal, T.A.; Goddard, W.A.; Jung, Y. Entropy and the driving force for the filling of carbon nanotubes with water. *Proceedings of the National Academy of Sciences* **2011**, *108*, 1108073108, doi:10.1073/pnas.1108073108.
42. Fu, Z.; Luo, Y.; Ma, J.; Wei, G. Phase transition of nanotube-confined water driven by electric field. *The Journal of Chemical Physics* **2011**, *134*, 154507, doi:10.1063/1.3579482.
43. Chakraborty, S.; Kumar, H.; Dasgupta, C.; Maiti, P.K. Confined Water: Structure, Dynamics, and Thermodynamics. *Accounts of Chemical Research* **2017**, *50*, 2139-2146, doi:10.1021/acs.accounts.6b00617.
44. Dalla Bernardina, S.; Paineau, E.; Brubach, J.-B.; Judeinstein, P.; Rouzière, S.; Launois, P.; Roy, P. Water in Carbon Nanotubes: The Peculiar Hydrogen Bond Network Revealed by Infrared Spectroscopy. *Journal of the American Chemical Society* **2016**, *138*, 10437-10443, doi:10.1021/jacs.6b02635.
45. Shayeganfar, F.; Beheshtian, J.; Shahsavari, R. First-Principles Study of Water Nanotubes Captured Inside Carbon/Boron Nitride Nanotubes. *Langmuir* **2018**, *34*, 11176-11187, doi:10.1021/acs.langmuir.8b00856.
46. Werkhoven, B.L.; van Roij, R. Coupled water, charge and salt transport in heterogeneous nano-fluidic systems. *Soft Matter* **2020**, *16*, 1527-1537, doi:10.1039/C9SM02144B.
47. Siria, A.; Poncharal, P.; Bianco, A.-L.; Fulcrand, R.; Blase, X.; Purcell, S.T.; Bocquet, L. Giant osmotic energy conversion measured in a single transmembrane boron nitride nanotube. *Nature* **2013**, *494*, 455-458, doi:10.1038/nature11876.
48. Zhang, L.; Chen, X. Nanofluidics for Giant Power Harvesting. *Angewandte Chemie International Edition* **2013**, *52*, 7640-7641, doi:10.1002/anie.201302707.
49. Choi, W.; Ulissi, Z.W.; Shimizu, S.F.E.; Bellisario, D.O.; Ellison, M.D.; Strano, M.S. Diameter-dependent ion transport through the interior of isolated single-walled carbon nanotubes. *Nature Communications* **2013**, *4*, 2397, doi:10.1038/ncomms3397.
50. Secchi, E.; Niguès, A.; Jubin, L.; Siria, A.; Bocquet, L. Scaling Behavior for Ionic Transport and its Fluctuations in Individual Carbon Nanotubes. *Physical Review Letters* **2016**, *116*, 154501, doi:10.1103/PhysRevLett.116.154501.
51. Su, J.; Guo, H. Control of Unidirectional Transport of Single-File Water Molecules through Carbon Nanotubes in an Electric Field. *ACS Nano* **2011**, *5*, 351-359, doi:10.1021/nn1014616.
52. Giovambattista, N.; Debenedetti, P.G.; Rosky, P.J. Effect of Surface Polarity on Water Contact Angle and Interfacial Hydration Structure. *The Journal of Physical Chemistry B* **2007**, *111*, 9581-9587, doi:10.1021/jp071957s.

- 544 53. Wang, C.; Lu, H.; Wang, Z.; Xiu, P.; Zhou, B.; Zuo, G.; Wan, R.; Hu, J.; Fang, H. Stable Liquid Water Droplet on a
545 Water Monolayer Formed at Room Temperature on Ionic Model Substrates. *Physical Review Letters* **2009**,
546 *103*, 137801, doi:10.1103/PhysRevLett.103.137801.
- 547 54. Wang, Z.; Ci, L.; Chen, L.; Nayak, S.; Ajayan, P.M.; Koratkar, N. Polarity-dependent electrochemically
548 controlled transport of water through carbon nanotube membranes. *Nano letters* **2007**, *7*, 697-702,
549 doi:10.1021/nl062853g.
- 550 55. Agrawal, B.; Singh, V.; Pathak, A.; Srivastava, R. Ab initio study of ice nanotubes in isolation or inside single-
551 walled carbon nanotubes. *Phys. Rev. B* **2007**, *75*, doi:10.1103/PhysRevB.75.195420.
- 552 56. Elliott, J.D.; Troisi, A.; Carbone, P. A QM/MD Coupling Method to Model the Ion-Induced Polarization of
553 Graphene. *Journal of Chemical Theory and Computation* **2020**, *16*, 5253-5263, doi:10.1021/acs.jctc.0c00239.
- 554 57. Otani, M.; Sugino, O. First-principles calculations of charged surfaces and interfaces: A plane-wave
555 nonrepeated slab approach. *Physical Review B* **2006**, *73*, 115407, doi:10.1103/PhysRevB.73.115407.
- 556 58. Amorim, R.G.; Fazzio, A.; Antonelli, A.; Novaes, F.D.; da Silva, A.J.R. Divacancies in Graphene and Carbon
557 Nanotubes. *Nano Letters* **2007**, *7*, 2459-2462, doi:10.1021/nl071217v.
- 558 59. Cohen-Tanugi, D.; Grossman, J.C. Water Desalination across Nanoporous Graphene. *Nano Letters* **2012**, *12*,
559 3602-3608, doi:10.1021/nl3012853.
- 560 60. Surwade, S.P.; Smirnov, S.N.; Vlassiouk, I.V.; Unocic, R.R.; Veith, G.M.; Dai, S.; Mahurin, S.M. Water
561 desalination using nanoporous single-layer graphene. *Nature Nanotechnology* **2015**, *10*, 459-464,
562 doi:10.1038/nnano.2015.37.
- 563 61. Sakong, S.; Kratzer, P. Hydrogen vibrational modes on graphene and relaxation of the C–H stretch excitation
564 from first-principles calculations. *The Journal of Chemical Physics* **2010**, *133*, 054505,
565 doi:10.1063/1.3474806.
- 566 62. Miura, Y.; Kasai, H.; Agerico Diño, W.; Nakanishi, H.; Sugimoto, T. Effective Pathway for Hydrogen Atom
567 Adsorption on Graphene. *Journal of the Physical Society of Japan* **2003**, *72*, 995-997,
568 doi:10.1143/JPSJ.72.995.
- 569 63. Yan, Z.; Zhu, L.; Li, Y.C.; Wycisk, R.J.; Pintauro, P.N.; Hickner, M.A.; Mallouk, T.E. The balance of electric field
570 and interfacial catalysis in promoting water dissociation in bipolar membranes. *Energy & Environmental*
571 *Science* **2018**, *11*, 2235-2245, doi:10.1039/C8EE01192C.
- 572 64. Cassone, G. Nuclear Quantum Effects Largely Influence Molecular Dissociation and Proton Transfer in Liquid
573 Water under an Electric Field. *The Journal of Physical Chemistry Letters* **2020**, *11*, 8983-8988,
574 doi:10.1021/acs.jpcllett.0c02581.
- 575 65. Saitta, A.M.; Saija, F.; Giaquinta, P.V. Ab Initio Molecular Dynamics Study of Dissociation of Water under an
576 Electric Field. *Physical Review Letters* **2012**, *108*, 207801, doi:10.1103/PhysRevLett.108.207801.
- 577 66. Muñoz-Santiburcio, D.; Marx, D. Nanoconfinement in Slit Pores Enhances Water Self-Dissociation. *Physical*
578 *Review Letters* **2017**, *119*, 056002, doi:10.1103/PhysRevLett.119.056002.
- 579 67. Sirkin, Y.A.P.; Hassanali, A.; Scherlis, D.A. One-Dimensional Confinement Inhibits Water Dissociation in
580 Carbon Nanotubes. *The Journal of Physical Chemistry Letters* **2018**, *9*, 5029-5033,
581 doi:10.1021/acs.jpcllett.8b02183.
- 582 68. Bepete, G.; Anglaret, E.; Ortolani, L.; Morandi, V.; Huang, K.; Pénicaud, A.; Drummond, C. Surfactant-free
583 single-layer graphene in water. *Nature Chemistry* **2017**, *9*, 347-352, doi:10.1038/nchem.2669.
- 584 69. Park, K.A.; Seo, K.; Lee, Y.H. Adsorption of Atomic Hydrogen on Single-Walled Carbon Nanotubes. *The Journal*
585 *of Physical Chemistry B* **2005**, *109*, 8967-8972, doi:10.1021/jp0500743.

- 586 70. Grosjean, B.; Bocquet, M.-L.; Vuilleumier, R. Versatile electrification of two-dimensional nanomaterials in
587 water. *Nature Communications* **2019**, *10*, 1656, doi:10.1038/s41467-019-09708-7.
- 588 71. Casolo, S.; Løvvik, O.M.; Martinazzo, R.; Tantardini, G.F. Understanding adsorption of hydrogen atoms on
589 graphene. *The Journal of Chemical Physics* **2009**, *130*, 054704, doi:10.1063/1.3072333.
- 590 72. Zhang, Z.W.; Zheng, W.T.; Jiang, Q. Hydrogen adsorption on Ce/SWCNT systems: a DFT study. *Physical*
591 *Chemistry Chemical Physics* **2011**, *13*, 9483-9489, doi:10.1039/C0CP02917C.
- 592 73. Ivanovskaya, V.V.; Zobelli, A.; Teillet-Billy, D.; Rougeau, N.; Sidis, V.; Briddon, P.R. Hydrogen adsorption on
593 graphene: a first principles study. *The European Physical Journal B* **2010**, *76*, 481-486,
594 doi:10.1140/epjb/e2010-00238-7.
- 595 74. Jena, N.K.; Tripathy, M.K.; Samanta, A.K.; Chandrakumar, K.R.S.; Ghosh, S.K. Water molecule encapsulated in
596 carbon nanotube model systems: effect of confinement and curvature. *Theoretical Chemistry Accounts* **2012**,
597 *131*, 1205, doi:10.1007/s00214-012-1205-z.
- 598 75. Matis, B.R.; Burgess, J.S.; Bulat, F.A.; Friedman, A.L.; Houston, B.H.; Baldwin, J.W. Surface Doping and Band
599 Gap Tunability in Hydrogenated Graphene. *ACS Nano* **2012**, *6*, 17-22, doi:10.1021/nn2034555.
- 600 76. Katin, K.P.; Prudkovskiy, V.S.; Maslov, M.M. Chemisorption of hydrogen atoms and hydroxyl groups on
601 stretched graphene: A coupled QM/QM study. *Physics Letters A* **2017**, *381*, 2686-2690,
602 doi:https://doi.org/10.1016/j.physleta.2017.06.017.
- 603 77. Lu, Y.; Feng, Y.P. Adsorptions of hydrogen on graphene and other forms of carbon structures: First principle
604 calculations. *Nanoscale* **2011**, *3*, 2444-2453, doi:10.1039/C1NR10118H.
- 605